Pharmaceutical Biology

ISSN: 1388-0209 (Print) 1744-5116 (Online) Journal homepage: informahealthcare.com/journals/iphb20

The combination of antitumor drugs, exemestane and erlotinib, induced resistance mechanism in H358 and A549 non-small cell lung cancer (NSCLC) cell lines

Ismini Kritikou, Efstathia Giannopoulou, Angelos K. Koutras, Vassiliki T. Labropoulou & Haralabos P. Kalofonos

To cite this article: Ismini Kritikou, Efstathia Giannopoulou, Angelos K. Koutras, Vassiliki T. Labropoulou & Haralabos P. Kalofonos (2014) The combination of antitumor drugs, exemestane and erlotinib, induced resistance mechanism in H358 and A549 non-small cell lung cancer (NSCLC) cell lines, Pharmaceutical Biology, 52:4, 444-452, DOI: 10.3109/13880209.2013.841718

To link to this article: https://doi.org/10.3109/13880209.2013.841718

Pharmaceutical Biology

http://informahealthcare.com/phb
ISSN 1388-0209 print/ISSN 1744-5116 online
Editor-in-Chief: John M. Pezzuto
Pharm Biol, 2014; 52(4): 444–452
 DOI: 10.3109/13880209.2013.841718

informa
healthcare

ORIGINAL ARTICLE

The combination of antitumor drugs, exemestane and erlotinib, induced resistance mechanism in H358 and A549 non-small cell lung cancer (NSCLC) cell lines

Ismini Kritikou[1], Efstathia Giannopoulou[1], Angelos K. Koutras[1,2], Vassiliki T. Labropoulou[1], and Haralabos P. Kalofonos[1,2]

[1]*Clinical Oncology Laboratory, University Hospital of Patras, Patras Medical School, Rion, Greece and* [2]*Division of Oncology, Department of Medicine, University Hospital of Patras, Rion, Greece*

Abstract

Context: Estrogens in non-small-cell lung cancer (NSCLC) are important, and their interaction with epidermal growth factor receptor (EGFR) might be crucial.
Objective: This study investigates the effect of exemestane, an aromatase inhibitor, and erlotinib, an EGFR inhibitor, on human NSCLC cell lines; H23, H358 and A549.
Materials and methods: A cell proliferation assay was used for measuring cell number, apoptosis assay for detecting apoptosis and necrosis and immunoblotting for beclin-1 and Bcl-2 proteins detection. An immunofluorescence assay was used for EGFR localization. A migration assay and zymography were used for cell motility and metalloproteinases (MMPs) expression, respectively.
Results: Exemestane, erlotinib or their combination decreased cell proliferation and increased apoptosis. Exemestane's half maximal inhibitory concentration (IC_{50}) was 50 μM for H23 and H358 cells and 20 μM for A549. The IC_{50} of erlotinib was 25 μM for all cell lines. Apoptosis increase induced by exemestane was 58.0 (H23), 186.3 (H358) and 34.7% (A549) and by erlotinib was 16.7 (H23), 65.3 (H358) and 66.3% (A549). A synergy effect was observed only in H23 cells. Noteworthy, the combination of exemestane and erlotinib decreased beclin-1 protein levels ($32.3 \pm 19.2\%$), an indicator of autophagy, in H23 cells. The combination of exemestane and erlotinib partially reversed the EGFR translocation to mitochondria and decreased MMP levels and migration.
Discussion and conclusions: The benefit from a dual targeting of aromatase and EGFR seems to be regulated by NSCLC cell content. The diverse responses of cells to agents might be influenced by the dominance of certain molecular pathways.

Keywords

Beclin-1, EGFR, migration, mitochondria

History

Received 14 January 2013
Revised 15 July 2013
Accepted 4 September 2013
Published online 5 November 2013

Introduction

Lung cancer remains a leading cause of cancer mortality. Approximately 85% of lung cancer cases are diagnosed with non-small-cell lung cancer (NSCLC). Survival of patients with NSCLC is still poor, and the future of effective treatment seems to be targeted therapies (Feld et al., 2006) with erlotinib, an epidermal growth factor receptor (EGFR) tyrosine kinase inhibitor (TKI) (Wang et al., 2008). Despite the promising action of TKIs, it is known in advance that all patients treated with gefitinib or erlotinib will develop drug resistance (Takeuchi & Ito, 2010). As such, it is of great importance to identify novel and effective combinations of agents based on molecular mechanisms in order to enhance the efficacy of TKIs.

Correspondence: H. P. Kalofonos, MD, PhD, Professor of Medical Oncology, Division of Oncology, Department of Medicine, University Hospital of Patras, Patras Medical School, Rion 26504, Greece. Tel: 0030-2610-999535. Fax: 0030-2610-994645. E-mail: kalofonos@upatras.gr

Exemestane is an irreversible steroidal aromatase inhibitor approved for postmenopausal women with breast cancer. The aromatase enzyme complex catalyses the final step in estrogen synthesis locally in tissues, including the lung. Although the estrogen pathway is well studied in breast cancer, its role in lung cancer has been investigated recently. New data from clinical trials showed a significant impact of hormone replacement therapy in lung cancer (Chlebowski et al., 2010; Garon et al., 2013; Slatore et al., 2010). Previous findings show that lung tumors express high levels of aromatase as well as estradiol, and its metabolites, and aromatase inhibition could be a useful therapeutic tool (Niikawa et al., 2008; Siegfried et al., 2009). Indeed, a case report of a 70-year-old female with lung adenocarcinoma during therapy with gefitinib showed enlarged lung nodules after 1-month treatment with estrogen (Siegfried et al., 2009; Wang et al., 2009). The aspect that inhibition of estrogen production might increase the efficacy of chemotherapy is interesting from a scientific viewpoint.

EGFR plays an important role in cell proliferation, survival, motility, angiogenesis and expression of extracellular matrix proteins. Furthermore, its function is deregulated in many types of malignancies (Takeuchi & Ito, 2010). The EGFR pathway is also regulated by numerous molecules that also participate in different pathways and engaged in yet unknown interactions. The interaction of the EGFR pathway with estrogen receptors (ERs) is a promising research area, which may help elucidate new aspects of EGFR signaling that depend on novel interactions. EGFR activation may lead to downstream protein kinase stimulation, such as mitogen-activated protein kinases and phosphatidylinositol 3-kinases (PI3K/Akt) and eventually in the stimulation of specific transcription factors. Given that it shares signaling molecules with the ER pathway, it may be involved in different interactions during signal transduction (Pietras et al., 2005).

Previous data from our laboratory showed that the administration of exemestane to NSCLC cell lines was associated with EGFR activation (Koutras et al., 2009). This observation was intriguing and warranted further examination of the interactions between the ER and EGFR molecular pathways. The aim of this study was to explore the benefits provided by the combined inhibition of aromatase and EGFR in NSCLC cells. We studied the effect of exemestane and erlotinib alone and in combination in cell proliferation and migration as well as their impact on molecules involved in cancer such as metalloproteinases (MMPs).

Materials and methods

Cell culture and reagents

NSCLC cell lines, H23, H358 and A549, and control breast cancer cell line, MCF-7, were purchased from the American Type Culture Collection (ATCC, LGC Standards, Wesel, Germany) and cultured as recommended by the manufacturer.

Aromatase inhibitor exemestane (Aromasin) and EGFR inhibitor erlotinib (Tarceva) were purchased by Pfizer (Hellas) and Roche (Hellas), respectively. Exemestane and erlotinib were applied to cell lines after cell attachment at doses of $1, 5, 10, 20$ and $50\,\mu M$ and $1, 10, 20, 25, 50$ and $100\,\mu M$, respectively. Both agents were diluted in dimethyl sulfoxide (DMSO). The final concentration of DMSO in culture medium was 0.5%. After reaching 50% confluence, cells were washed with phosphate buffer saline (PBS) and incubated with phenol red-free medium with 1% dextran-coated, charcoal-treated fetal bovine serum (FBS) (working medium) for 24 h to deplete estrogen (Weinberg et al., 2005). All the experiments were performed according to these conditions. Thereafter, cells were treated with exemestane or erlotinib at the indicated time points and doses.

Cell proliferation assay

To determine whether exemestane, erlotinib or their combination affect the proliferation of H23, H358 and A549 cells, the 3-[4,5-dimethylthiazol-2-yl]-2,5-dimethyltetrazolium bromide (MTT) assay was used as previously described (Giannopoulou et al., 2009a). Briefly, cells were seeded at a density of 2×10^4 cells/well in 24-well plates with working medium. Cells were treated with each agent alone and/or in combination for 48 h. MTT solution (5 mg/ml in PBS) was prepared, and a volume equal to 1/10 was added to each well and incubated for 2 h at 37 °C. Medium was removed and 100 µl acidified isopropanol (0.33 ml HCl in 100 ml isopropanol) was added in each well in order solubilize the dark blue formazan crystals. The solution was transferred to 96-well plates and immediately read in a microplate reader (Tecan Sunrise, Magellan 2, Grodig, Austria) at a wavelength of 570 nm using reference wavelength 620 nm.

Apoptosis assay

All cell lines were plated at 1×10^5 cells per well in six-well plates. Agents were added as described above. At the end of a 48-h incubation, cells were washed twice with PBS, trypsinized for 7 min and centrifuged for 4 min at $166\,g$. Cells were resuspended in 200 µl $1 \times$ binding buffer (10 mM hydroxyethylpiperazine ethane sulfonic acid pH 7.4, 140 mM NaCl and 2.5 mM $CaCl_2$). The cell suspension was incubated with 5 µl Annexin V-FITC in the dark at 25 °C for 10 min. Then, 10 µl of the 20 µg/ml propidium iodide stock solution was added, followed by 200 µl of binding buffer, and the cells were immediately analyzed by flow cytometry (Kuwada et al., 2004) (EPICS-XL of Coulter) according to the manufacturer's instructions (rh Annexin V/FITC kit, Bender MedSystems, Vienna, Austria).

Immunoblotting

Cells were plated on Petri dishes. After reaching 80% confluence, cells were treated with working medium, as described above. Forty-eight hours after drug addition, cells were collected with scrapper and lysed using lysis buffer (50 mM Tris-HCl pH 7.5, 150 mM NaCl, 5 mM EDTA, 1% Triton, 10% glycerol, 1 mM phenylmethylsulfonyl fluoride, 2 mM Na-orthovanadate and 10 mM leupeptin). Protein concentration was determined by the Bradford assay. Samples were analyzed by immunoblotting as previously described (Giannopoulou et al., 2009a). A goat polyclonal anti-Beclin-1 (dilution 1:500, Santa Cruz, CA), a monoclonal anti-Bcl-2 (dilution 1:500, Santa Cruz, CA) and a monoclonal anti-actin antibody (dilution 1:1000, Chemicon, Millipore, Temecula, CA) were used.

Detection of the immunoreactive proteins was performed by chemiluminescence using horseradish peroxidase substrate SuperSignal (Pierce, Rockford, IL), according to the manufacturer's instructions.

Migration assay

Migration assays were performed as previously described (Hede, 2007) in 24-well microchemotaxis chambers (Costar, Avon, France), using uncoated polycarbonate membranes with 8 µm pores. The cells that migrated through the filter were quantified by counting the entire area of each filter, using a grid and a microscope at a $20 \times$ magnification.

Zymography

The release of MMP-9 and MMP-2 into the culture medium of H23, H358 and A549 cells was measured by zymography as previously described (Hede, 2007). In brief, cells were plated in

24-well plates at a density of 3×10^4 cells per well in working medium. The cells were treated with the tested agents, as described above for the proliferation studies. Forty-eight hours later, 50 µl of the medium from each group were diluted with 2× Laemmli sample buffer without β-mercaptoethanol. Protein concentration was detected using the Bradford assay, and equals amounts of total proteins were analyzed. Samples from both cell lines were analyzed in 10% sodium dodecyl sulfate polyacrylamide gel electrophoresis gels containing 0.1% gelatin. Following electrophoresis, gels were washed four times in 2.5% Triton-X 100 for 15 min at room temperature and incubated for 24 h at 37 °C in developing buffer (50 mM Tris-HCl pH 7.6, 200 mM NaCl and 10 mM $CaCl_2$). The gels were stained with Coomassie Brilliant Blue R for 4 h at room temperature, de-stained in methanol–acetic acid–water (4.5:1:4.5 v/v) for 2 h and photographed using a digital camera.

Immunofluorescence

All cell lines were treated with drugs as previously described. Twenty-four hours later, medium was removed and cells were washed twice with PBS. Dye for mitochondria (25 nM, MitoTracker Red, Invitrogen, Molecular Probe, Eugene, OR) was added to cells in culture 45 min prior to cell fixation. Cells were fixed with a 4% *p*-formaldehyde in PBS buffered solution for 30 min at room temperature and then they were rinsed 3 × 5 min with PBS. An incubation of 1 h at 37 °C in a 3% BSA in PBS solution supplemented with 10% FBS followed. After the incubation with blocking solution, cells were rinsed once with PBS for 5 min and they were treated overnight at 4 °C with a monoclonal anti-EGFR antibody diluted in blocking solution (10 µg/ml, Upstate, Lake Placid, NY). Cells were rinsed 3 × 5 min with PBS and then an anti-mouse antibody conjugated with Alexa Fluor 488 (1:500, Invitrogen, Molecular probe) diluted in blocking solution was added for 30 min at 37 °C. Cells were rinsed 3 × 5 min with PBS and mounted on glass sides. Fluorescence was visualized using a Leica microscope (Leica TCS SP5, Mannheim, Germany) at 63 × magnification.

Statistical analysis

Differences between groups and controls were tested by one-way analysis of variance. Each experiment included at least triplicate measurements. All results are expressed as mean ± SEM from at least three independent experiments.

Results

Aromatase expression in H23, H358 and A549 cells

H23 cells express low levels of aromatase, H358 express moderate and A549 express high levels (data not shown).

Exemestane, erlotinib and their combination reduced H23, H358 and A549 cell number and increased apoptosis

We studied the effect of exemestane and erlotinib on the proliferation of H23, H358 and A549 cells. Exemestane inhibited cell proliferation in all cell lines in a dose-dependent manner, 48 h after its application, consistent with previous results from our group (Koutras et al., 2009) (Figure 1a). Fifty percent growth inhibition was recorded at 50 µM for H23 and H358 and 20 µM for A549. Erlotinib inhibited cell proliferation, in a similar way, in all cell lines in a dose-dependent manner, 48 h after its application (Figure 1b). Fifty percent growth inhibition was recorded at 25 µM for H23, H358 and A549 cell lines. All further experiments for each cell line were performed with these concentrations of exemestane and erlotinib.

We next studied the effect of agent combination on cell numbers. The combined administration of exemestane and erlotinib reduced cell numbers in all cell lines examined in this study. However, inhibitor synergy was identified only in H23 cells according to a formula that Fischel et al. (2005) previously described (Figure 1c, d, e).

Furthermore, the percentage of annexin$^+$ in cells increased 48 h after treatment of H23, H358 or A549 with exemestane, erlotinib and their combination, compared to untreated cells (Table 1). The increase in cell apoptosis was in line with the decrease of the anti-apoptotic protein Bcl-2 as shown in Figure 2 for the three cell lines. Bcl-2 protein was detected 24 h after agent application, and we found a decreased trend in H23 cells by exemestane (7.7 ± 5.3), a strong decrease by erlotinib (28.0 ± 0.7) as well as by the agent in combination (58.3 ± 5.7). A trend decrease was found in H358 cells, by exemestane (5.2 ± 2.9), erlotinib (21.9 ± 19.9) and their combination (14.1 ± 8.9). Similarly, in A549 cells, exemestane (59.8 ± 8.8) and erlotinib (21.9 ± 11.2) decreased Bcl-2 protein as well as their combination (11.9 ± 5.5). No effect was observed on cell necrosis or on the distribution of cells in the phases of cell cycle (data not shown).

Effect of exemestane and erlotinib on beclin-1 protein levels

Beclin-1 protein levels were measured in order to determine the effect of the inhibitors on cell autophagy (Giannopoulou et al., 2009b). In H23 cells, an increase of beclin-1 (24.3 ± 6.8) was observed 24 h after exemestane application (Figure 3). An increase trend was demonstrated in H23 after erlotinib application (17.6 ± 10.6) without, however, being statistically significant. Surprisingly, erlotinib reversed the increasing action of exemestane when their combination was applied in the same cells (32.3 ± 19.2). No changes were observed in A549 or H358 cells (Figure 3).

Effect of exemestane and erlotinib on cell migration

We next studied the effects of exemestane, erlotinib and their combination on cell migration. Compared to the untreated cells, each agent alone or their combination inhibited H23 cell migration (Figure 4a), 4 h after their application. In H358 cells, only exemestane exerted an inhibitory effect (Figure 4b), and this effect was reversed when both agents were applied. No changes were observed in the ability of A549 cells to migrate when the inhibitors alone or in combination was applied (data not shown).

Effect of the inhibitors on MMPs secretion

The effect of exemestane, erlotinib and their combination on the secretion of MMP-2 and MMP-9 in cell supernatant was studied, 48 h after their application.

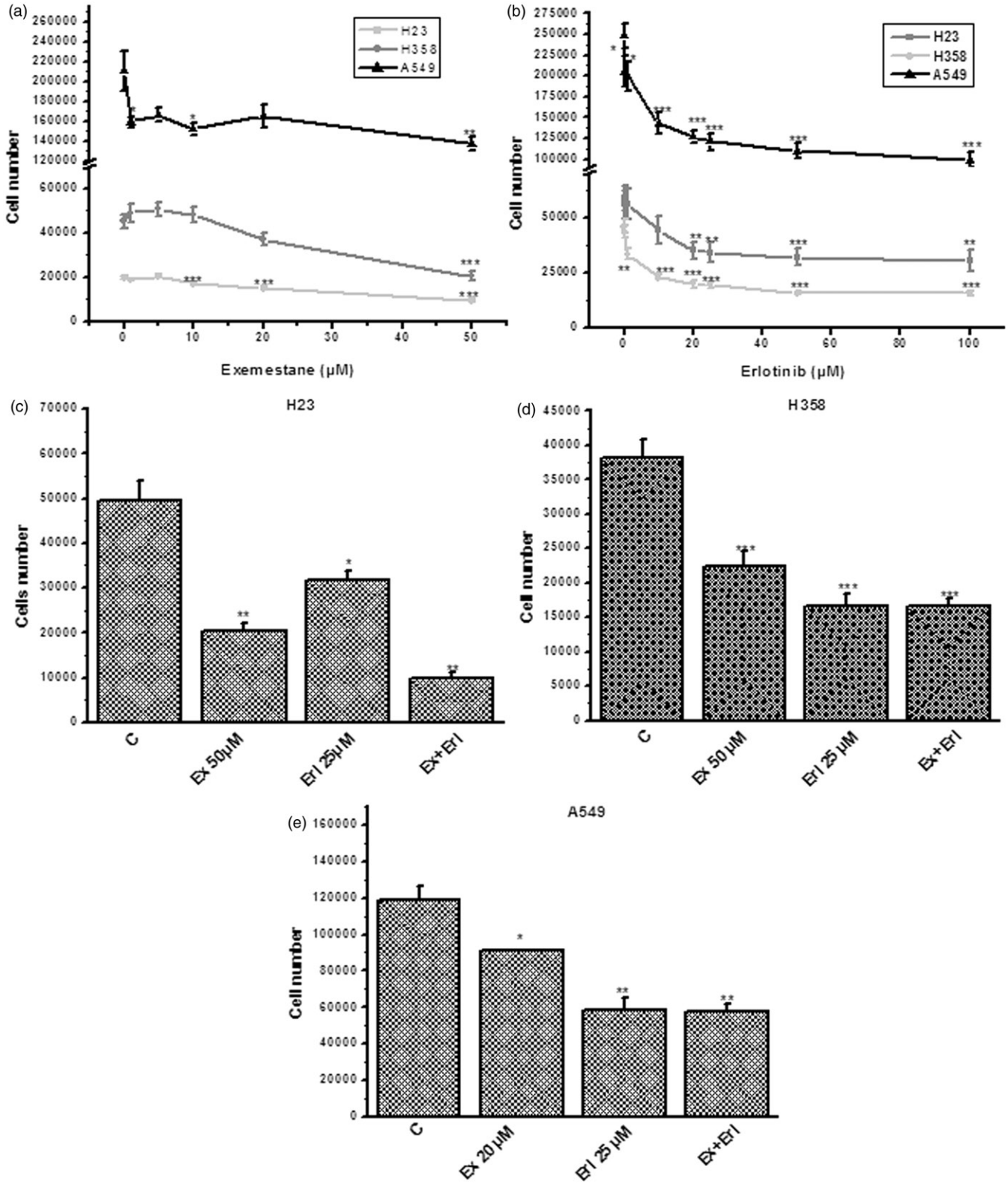

Figure 1. Dose-response of (a) exemestane and (b) erlotinib of H23, H358 and A549 cells. Different doses of exemestane or erlotinib were applied on cell lines; and 48 h later, cell number was estimated by colorimetric MTT assay. Combined targeting of aromatase and EGFR with exemestane and erlotinib on (c) H23, (d) H358 and (e) A549, respectively, 48 h after drug application. The results were expressed as cell number ± SEM. Asterisks denote a statistically significant difference compared to untreated cells. $*p<0.05$, $**p<0.01$ and $***p<0.001$. C: control, Ex: exemestane, Erl: erlotinib and Ex + Erl: exemestane and erlotinib.

Exemestane reduced MMP secretion in the H23 cell line (Figure 5). A similar effect was observed when the combination was applied. MMP secretion was not changed by the inhibitors in H358 and A549 cells (Figure 5).

Localization of EGFR in H23, H358 and A549 cells

We evaluated the effect of exemestane on EGFR localization. In H23 cells, we found that EGFR translocated from the cell

Table 1. The effect of exemestane and erlotinib on apoptosis of H23, H358 and A549 cells.

	H23		H358		A549	
Apoptosis 48 h (%)	%	*p*	%	*p*	%	*p*
Ex.	58.0 ± 26.0	0.025[a]	186.3 ± 13.7	0.00017[b]	34.7 ± 13.4	0.018[a]
Erl.	16.7 ± 5.0	0.023[a]	65.3 ± 14.4	0.0105[a]	66.3 ± 13.6	0.00816[c]
Ex + Erl	44.0 ± 8.5	0.0064[c]	406.3 ± 16.5	0.000017[b]	37.7 ± 26.8	0.031[a]

Results are expressed as the % percentage of annexin$^+$ cells ± SEM compared to untreated cells based on at least three independent experiments. Asterisks denote a statistically significant difference compared to untreated cells (C).
[a]$p < 0.05$.
[b]$p < 0.001$.
[c]$p < 0.01$.
Ex: exemestane, Erl: erlotinib, Ex + Erl: exemestane + erlotinib.

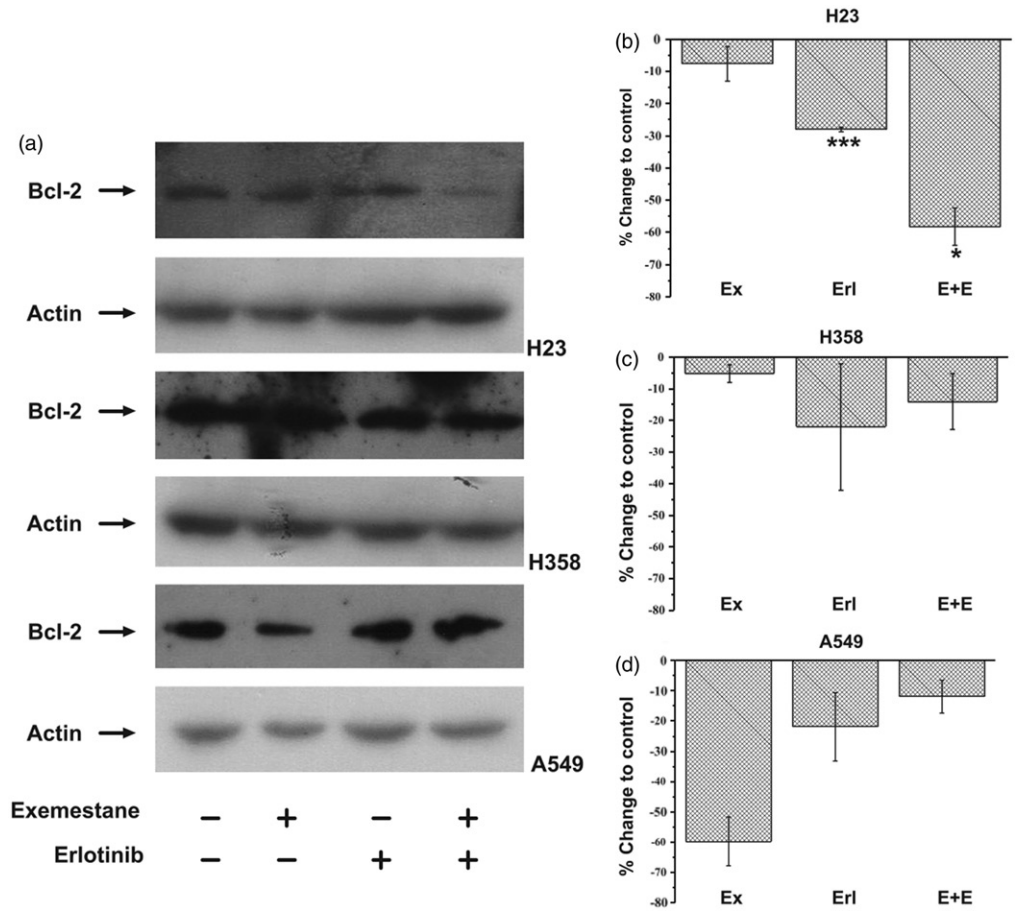

Figure 2. The effect of exemestane, erlotinib and their combination on Bcl-2 anti-apoptotic protein levels. (a) Representative blots of three independent experiments for H23, H358 and A549 cells. Quantification of western blot images (b) in H23, (c) in H358 and (d) in A549. Results are expressed as mean ± SEM of the % change compared to the untreated cells. Asterisks denote a statistically significant difference compared to untreated cells. *$p < 0.05$ and ***$p < 0.0001$. C: control, Ex: exemestane, Erl: erlotinib and E + E: exemestane and erlotinib.

membrane into mitochondria, 24 h after the addition of each agent alone, while their combination reversed partially this effect (Figure 6). However, in H358 and A549 cells, no changes in EGFR localization were demonstrated following the treatment of cells with exemestane, erlotinib or their combination (data not shown).

Discussion

In this study, we investigated the combined effects of exemestane and erlotinib on NSCLC cell line proliferation, apoptosis, migration and autophagy. First, we studied the effect of the combination of exemestane and erlotinib on cell proliferation. Both agents exerted an antitumor effect on all cell lines, revealing, however, inhibitor synergy only in the H23 cell line. The fact that synergy is observable only in H23 cells that express the lowest aromatase protein levels among the three cell lines might imply a different mechanism of agent action in these cells. Moreover, increased cell apoptosis in association with a decrease in anti-apoptotic protein Bcl-2 in all cell lines by each agent, alone or their combination, indicate apoptosis as the mechanism of cell

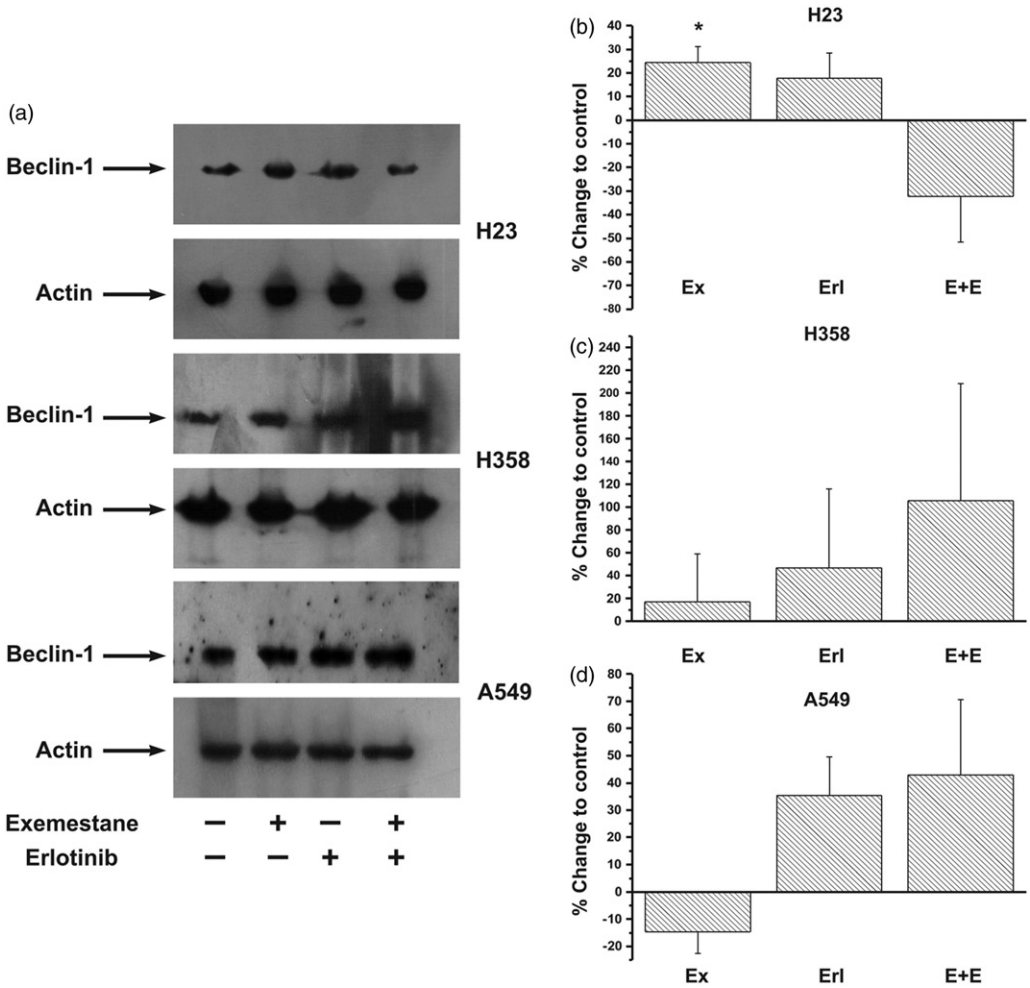

Figure 3. The effect of exemestane and erlotinib on beclin-1 protein levels. (a) Representative blots of three independent experiments for H23, H358 and A549 cells. Quantification of western blot images (b) in H23, (c) in H358 and (d) in A549. Results are expressed as mean ± SEM of the % change compared to the untreated cells. Asterisks denote a statistically significant difference compared to untreated cells. $*p<0.05$. C: control, Ex: exemestane, Erl: erlotinib, E + E: exemestane and erlotinib.

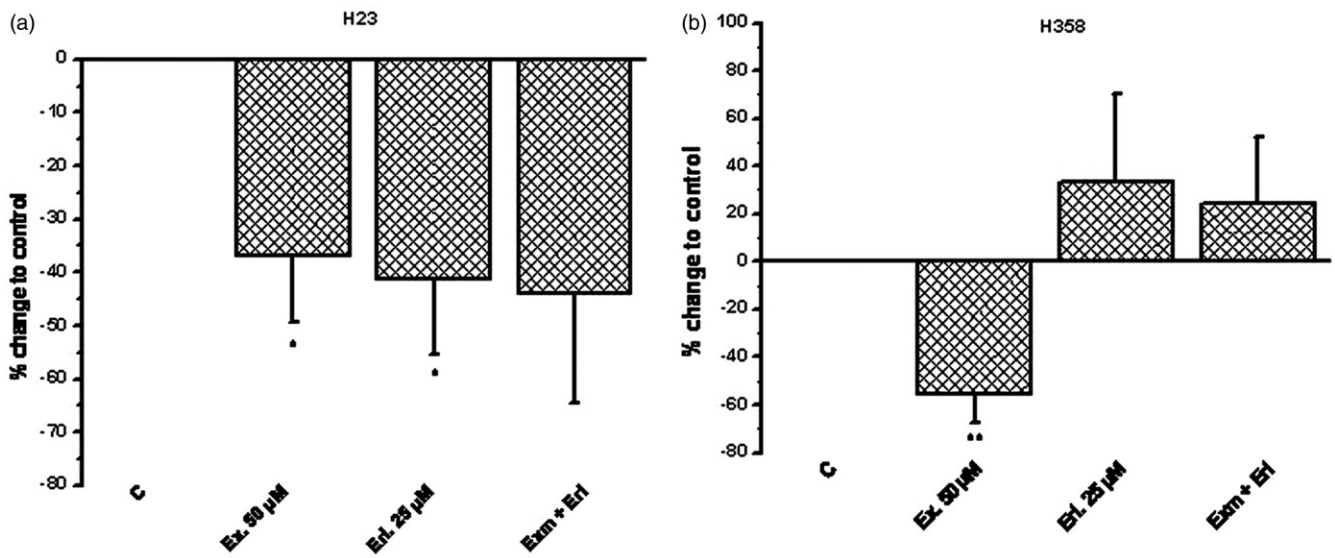

Figure 4. The effect of exemestane and erlotinib on H23 (a) and H358 (b) migration ability. Results are expressed as mean ± SEM of the % change compared to the untreated cells. Asterisks denote a statistically significant difference compared to untreated cells. $*p<0.05$ and $**p<0.01$. C: control, Ex: exemestane, Erl: erlotinib, E + E: exemestane and erlotinib.

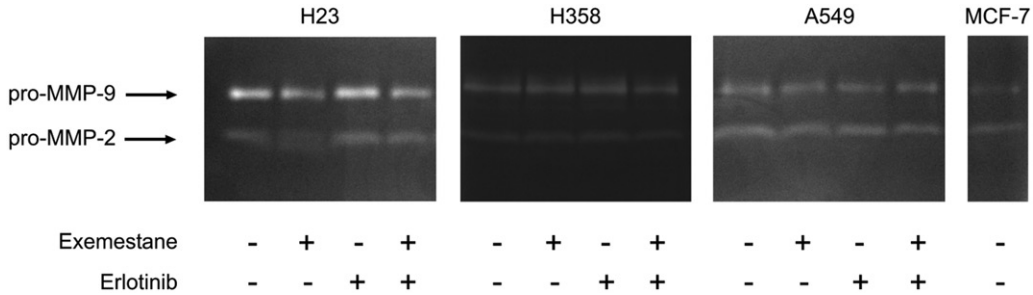

Figure 5. Effect of exemestane and erlotinib on MMP-9 and MMP-2 secretion by H23, H358 and A549 cells. This picture is a representative gel of three independent experiments.

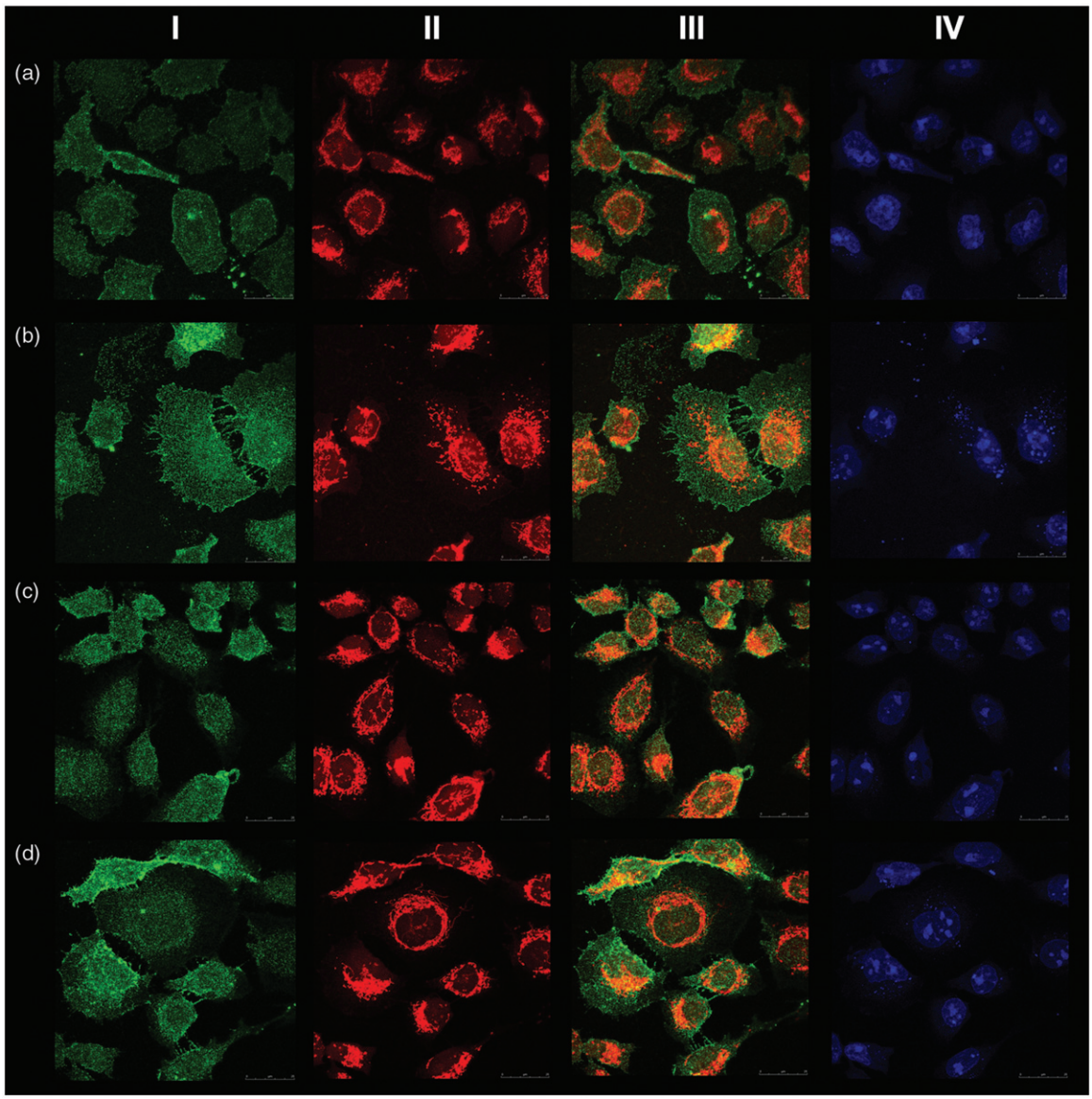

Figure 6. The effect of exemestane and erlotinib on EGFR localization in H23 cells at the time point of 24 h after drug application. Untreated cells (a) and cells treated with exemestane (b), erlotinib (c) and their combination (d) were stained with anti-EGFR (I), mitochondria dye (II) and nucleus dye (III) and visualized in confocal microscope. The colocalization for three fluorescent dyes is demonstrated in lane (IV). The figure is a representative of at least three independent experiments using a magnification of 63×.

number reduction. These antiproliferative effects are in line with previous data (Stabile et al., 2005), which indicate greater antitumor effects with the combined targeting of ER and EGFR in several lung cancer cells except for A549. Stabile et al., in this study, suggested that the mutational status of EGFR is the reason for this difference. However, in our study, this seems not to be the case, because all our cell lines express wild type EGFR. We might assume that the molecular profiling could help elucidate the differences among the cell lines. H358 and A549 cells express wild-type

phosphatase and tensin homolog (PTEN), while H23 are PTEN mutant and, therefore, express high Akt levels due to the increased PI3K pathway activation (Yoon et al., 2010). In H23 cells with mutated PTEN renders PI3K the main pathway that regulates cell proliferation (Scaltriti & Baselga, 2006). Apart from EGFR, the PI3K pathway is also regulated by ER signaling (Johnston, 2009; Osborne et al., 2001; Stabile & Siegfried, 2004). The absence of control for the PI3K/Akt pathway due to mutated PTEN might render the H23 cells more vulnerable to combined inhibition of the EGFR and ER pathways. This could explain the observed synergy in H23 cells.

Moreover, the mutational status of PTEN might explain the effect of the inhibitors on MMP secretion. The PI3K pathway also regulates MMP secretion (Meng et al., 2009), assuming that the mutated PTEN allows the PI3K to be the major pathway for the regulation of MMP secretion in H23 cells. Thus, the inhibition of PI3K pathway, caused by exemestane, resulted in decreased MMP levels.

Another type of influence of the tested agents on tumor cell invasiveness is suggested by their effects on cell migration. In H23 cells, both agents as well as their combination inhibited the ability of the cells to migrate. In H358, exemestane inhibited cell migration. No effect was observed in A549 cells. Mase et al. categorized several lung cancer cell lines according to their tumorigenicity and ranked H23 in the group with low incidence of intrapulmonary implantations and H358 and A549 in the group with high incidence of intrapulmonary implantations (Mase et al., 2002). The observed sensitivity of H23 and the relative resistance of H358 and A549 cells could explain their differences in metastatic capacity. Furthermore, the same research group found that the A549 cells developed both high incidence of intrapulmonary implantation and lymph node metastasis, while the H358 did not develop any lymph node metastasis. Although the reason for this difference is not known, it is likely for those cell lines to have different molecular profiles that could explain the sensitivity of H358 and the resistance of A549 to exemestane, respectively.

Translocation of EGFR into the mitochondria was observed in the H23 cell line 24 h after the application of each agent alone or combined. Except for the plasma membrane, EGFR has been found in several cell organelles, including the mitochondria (Lin et al., 2001). It has been recently suggested that autophagy promotes EGFR mitochondrial translocation, leading to cell survival (Yue et al., 2008). This is, therefore, a possible justification for the EGFR mitochondrial translocation mentioned above. This suggestion is supported by the increase of beclin-1, an autophagy indicator (Giannopoulou et al., 2009), that was detected after treatment of H23 cells with exemestane or erlotinib. However, when the combination of exemestane and erlotinib was applied, EGFR translocation partially reversed, and this is in line with the decrease in beclin-1 protein levels. The role of autophagy is complicated in cancer and varies among the cell types leading to cell death or survival. Although the most antitumor agents stimulate autophagy contributing to cell death, there are agents such as rapamycin (sirolimus) that activate autophagic processes (Lefranc et al., 2007). Thus, this is not the first time that an antitumour agent may activate autophagy. However, the combination of agents may reverse this procedure. Previous data showed that 2-deoxyglucose induced autophagy, while when it was combined with metformin, this effect was reversed (Ben Sahra et al., 2010).

Conclusions

Although the dual targeting of aromatase and EGFR could induce resistance in certain cell lines, they could be effective in cells with a defined molecular profile. The EGFR pathway activation that might offer a resistance to H358 and A549 cells but not in H23 cells is very important for setting the basis for patient selection that might gain benefit from dual targeting of aromatase and EGFR. The contribution of aromatase inhibitors in the therapeutic option for patients with NSCLC in the future has been discussed recently (Verma et al., 2011). Detailed gene and/or protein profile analysis might contribute to identify differences in EGFR related pathways and could point to combined and targeted approaches with the aim of overcoming the resistance mechanisms that operate in the current treatment.

Acknowledgements

We would like to thank the Medical School, University of Patras, Greece, for providing us the Advanced Light Microscopy facility, EOGE Oncological Research Fund for financial support and Gregoris Iconomou, PhD, Quality of life Unit, Division of Oncology, University Hospital of Patras, Greece for linguistic editing.

Declaration of interest

The authors report no declarations of interest.

References

Ben Sahra I, Laurent K, Giuliano S, et al. (2010). Targeting cancer cell metabolism: The combination of metformin and 2-deoxyglucose induces p53-dependent apoptosis in prostate cancer cells. *Cancer Res* 70:2465–75.

Chlebowski RT, Anderson GL, Manson JE, et al. (2010). Lung cancer among postmenopausal women treated with estrogen alone in the women's health initiative randomized trial. *J Natl Cancer Inst* 102: 1413–21.

Feld R, Sridhar SS, Shepherd FA, et al. (2006). Use of the epidermal growth factor receptor inhibitors gefitinib and erlotinib in the treatment of non-small cell lung cancer: A systematic review. *J Thorac Oncol* 1:367–76.

Fischel JL, Formento P, Milano G. (2005). Epidermal growth factor receptor double targeting by a tyrosine kinase inhibitor (Iressa) and a monoclonal antibody (Cetuximab). Impact on cell growth and molecular factors. Br J Cancer 92:1063–8.

Garon EB, Pietras RJ, Finn RS, et al. (2013). Antiestrogen fulvestrant enhances the antiproliferative effects of epidermal growth factor receptor inhibitors in human non-small-cell lung cancer. *J Thorac Oncol* 8:270–8.

Giannopoulou E, Antonacopoulou A, Floratou K, et al. (2009a). Dual targeting of EGFR and HER-2 in colon cancer cell lines. *Cancer Chemother Pharmacol* 63:973–81.

Giannopoulou E, Antonacopoulou A, Matsouka P, Kalofonos HP. (2009b). Autophagy: Novel action of panitumumab in colon cancer. *Anticancer Res* 29:5077–82.

Hede K. (2007). Lung cancer may be different for men and women, but researchers ponder what to do? *J Natl Cancer Inst* 99:1830–2.

Johnston SR. (2009). Enhancing the efficacy of hormonal agents with selected targeted agents. *Clin Breast Cancer 9 Suppl* 1:S28–36.

Koutras A, Giannopoulou E, Kritikou I, et al. (2009). Antiproliferative effect of exemestane in lung cancer cells. *Mol Cancer* 8:109.

Kuwada SK, Scaife CL, Kuang J, et al. (2004). Effects of trastuzumab on epidermal growth factor receptor-dependent and -independent human colon cancer cells. *Int J Cancer* 109:291–301.

Lefranc F, Facchini V, Kiss R. (2007). Proautophagic drugs: A novel means to combat apoptosis-resistant cancers, with a special emphasis on glioblastomas. *Oncologist* 12:1395–403.

Lin SY, Makino K, Xia W, et al. (2001). Nuclear localization of EGF receptor and its potential new role as a transcription factor. *Nature Cell Biol* 3:802–8.

Mase K, Iijima T, Nakamura N, et al. (2002). Intrabronchial orthotopic propagation of human lung adenocarcinoma – Characterizations of tumorigenicity, invasion and metastasis. *Lung Cancer* 36:271–6.

Meng XN, Jin Y, Yu Y, et al. (2009). Characterisation of fibronectin-mediated FAK signalling pathways in lung cancer cell migration and invasion. *Br J Cancer* 101:327–34.

Niikawa H, Suzuki T, Miki Y, et al. (2008). Intratumoral estrogens and estrogen receptors in human non-small cell lung carcinoma. *Clin Cancer Res* 14:4417–26.

Osborne CK, Schiff R, Fuqua SA, Shou J. (2001). Estrogen receptor: Current understanding of its activation and modulation. *Clin Cancer Res* 7:4338s–42s; discussion 4411s–2s.

Pietras RJ, Marquez DC, Chen HW, et al. (2005). Estrogen and growth factor receptor interactions in human breast and non-small cell lung cancer cells. *Steroids* 70:372–81.

Scaltriti M, Baselga J. (2006). The epidermal growth factor receptor pathway: A model for targeted therapy. *Clin Cancer Res* 12: 5268–72.

Siegfried JM, Hershberger PA, Stabile LP. (2009). Estrogen receptor signaling in lung cancer. *Semin Oncol* 36:524–31.

Slatore CG, Chien JW, Au DH, et al. (2010). Lung cancer and hormone replacement therapy: Association in the vitamins and lifestyle study. *J Clin Oncol* 28:1540–6.

Stabile LP, Lyker JS, Gubish CT, et al. (2005). Combined targeting of the estrogen receptor and the epidermal growth factor receptor in non-small cell lung cancer shows enhanced antiproliferative effects. *Cancer Res* 65:1459–70.

Stabile LP, Siegfried JM. (2004). Estrogen receptor pathways in lung cancer. *Curr Oncol Rep* 6:259–67.

Takeuchi K, Ito F. (2010). EGF receptor in relation to tumor development: Molecular basis of responsiveness of cancer cells to EGFR-targeting tyrosine kinase inhibitors. *FEBS J* 277:316–26.

Verma MK, Miki Y, Sasano H. (2011). Aromatase in human lung carcinoma. *Steroids* 76:759–64.

Wang PH, Wang HC, Tsai CC. (2009). Estrogen replacement in female lung cancer during gefitinib therapy. *Jpn J Clin Oncol* 39: 829–32.

Wang YC, Kulp SK, Wang D, et al. (2008). Targeting endoplasmic reticulum stress and Akt with OSU-03012 and gefitinib or erlotinib to overcome resistance to epidermal growth factor receptor inhibitors. *Cancer Res* 68:2820–30.

Weinberg OK, Marquez-Garban DC, Fishbein MC, et al. (2005). Aromatase inhibitors in human lung cancer therapy. *Cancer Res* 65: 11287–91.

Yoon YK, Kim HP, Han SW, et al. (2010). KRAS mutant lung cancer cells are differentially responsive to MEK inhibitor due to AKT or STAT3 activation: Implication for combinatorial approach. *Mol Carcinog* 49:353–62.

Yue X, Song W, Zhang W, et al. (2008). Mitochondrially localized EGFR is subjected to autophagic regulation and implicated in cell survival. *Autophagy* 4:641–9.